

PARTICLE TRACKING FOR THE FETS LASER WIRE EMITTANCE SCANNER

J. Pozimski, Imperial College, London, UK
 S. Gibson, RHUL, London, UK

Abstract

The Front End Test Stand (FETS) is an R&D project at Rutherford Appleton Laboratory (RAL) with the aim to demonstrate a high power (60 mA, 3 MeV with 50 pps and 10 % duty cycle), fast chopped H⁻ ion beam. The diagnostics of high power particle beams is difficult, due to the power deposition on diagnostics elements introduced in the beam, so non-invasive instrumentation is highly desirable. The laser wire emittance scanner under construction is based on a photo-detachment process, utilizing the neutralized particles produced in the interaction between Laser and H⁻ beam for beam diagnostics purposes. The principle is appropriate to determine the transversal beam density distribution, as well as the transversal and longitudinal beam emittance behind the RFQ. The instrument will be located at the end of the MEBT with the detachment taking place inside a dipole field. Extensive particle tracking simulations have been performed for various settings of the MEBT quadrupoles to investigate the best placement and size of the 2D scintillating detector, and to determine the range and resolution of the instrument. Additionally the power distribution in the following beam dumps has been determined.

INTRODUCTION

In order to contribute to the development of high power proton accelerators in the MW range, to prepare the way for an ISIS upgrade and to contribute to the UK design effort on neutrino factories, a front end test stand (FETS) is being constructed at the Rutherford Appleton Laboratory (RAL) in the UK [1,2]. The aim of the FETS is to demonstrate the production of a 60 mA, 2 ms, 50 pps chopped beam at 3 MeV with sufficient beam quality. FETS consists of a high brightness ion source [3] and a magnetic 3 solenoid LEPT [4], both of which are operational. [2]. A 4-vane 324MHz radio frequency quadrupole [5] accelerating the beam to 3 MeV is

manufactured and will be assembled and tested in the next month. Following the RFQ is the medium energy beam transport (MEBT) [6], containing a high speed beam chopper [7] and non-destructive photo-detachment diagnostics. The MEBT is in the design phase; with the particle dynamics design finished and the transition to the mechanical design started. The layout of FETS is shown in Fig. 1.

While the original aim of FETS was the test of the fast/slow chopper scheme, in 2005 while FETS was still in an early stage it was decided to include tests of laser based beam diagnostics (LD). The concept of the envisaged laser wire emittance scanner to be realized at FETS is based on the experiments on this subject performed at Frankfurt University [8, 9]. While the most appropriate position for these experiments on FETS has been identified to be after the RFQ for reasons of residual gas pressure and the time structure of the ion beam [10], the overall time schedule for FETS allowed for pre experiments using a laserwire setup at the beginning of the LEPT to investigate the beam profile shortly after post acceleration [11, 12].

The final part of the FETS MEPT (Fig. 1 red box) is now to be optimized to allow for the test of the laser based beam diagnostics (LD) under construction. A more detailed layout of the MEPT section under design for the Laser wire emittance scanner is shown in Fig. 2. It consists of the main beam dump in straight forward direction (1), a quadrupole duplet (2) to diffuse the beam after the LD dipole, the laser delivery system (3), a quadrupole duplet (and optional rebunching cavity) (4) at the entrance to the LD dipole, the LD dipole to separate the neutralized particles from the beam ions (5) and a quadrupole duplet (6) in front of the secondary beam dump (7). Barely visible from the shown perspective between the beam dumps is the particle detector (scintillator) for the neutralized atoms and CCD camera for readout (8).

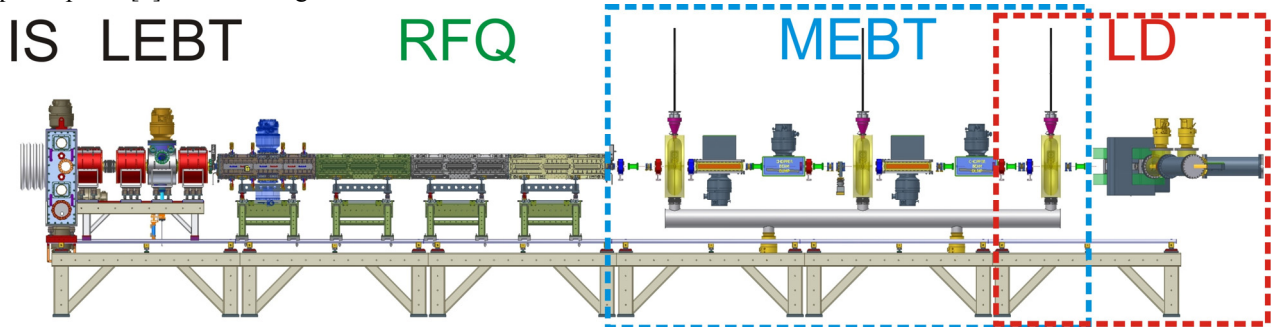


Figure 1: Schematic layout of the Front end test stand at RAL consisting of (left to right) ion source, LEPT, 4 vane RFQ, MEPT with fast & slow chopper followed by the laser diagnostic section.

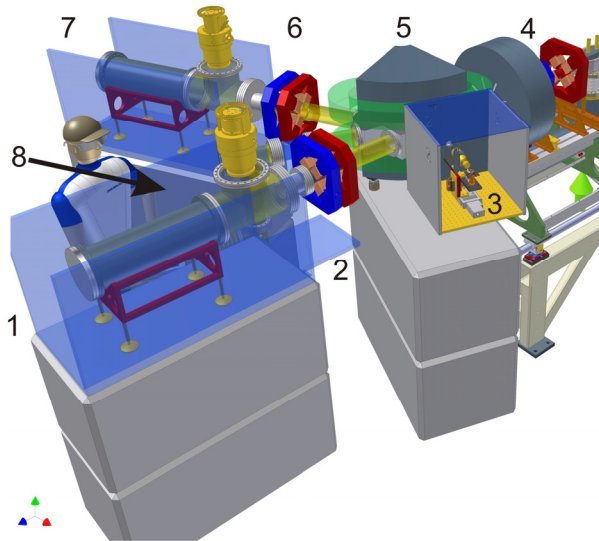


Figure 2: Details of the LD set up defining the lattice for the particle tracking. See text for further explanation.

PARTICLE TRACKING SETUP

The particle tracking has been performed using the general particle tracer GPT [13]. A first simulation from the exit of the RFQ to the end of the chopping section at 4.13 m was performed to produce the input distribution (shown in Fig. 3) for the following simulations.

position in z = 4.13 m
N(nmacro) = 95132

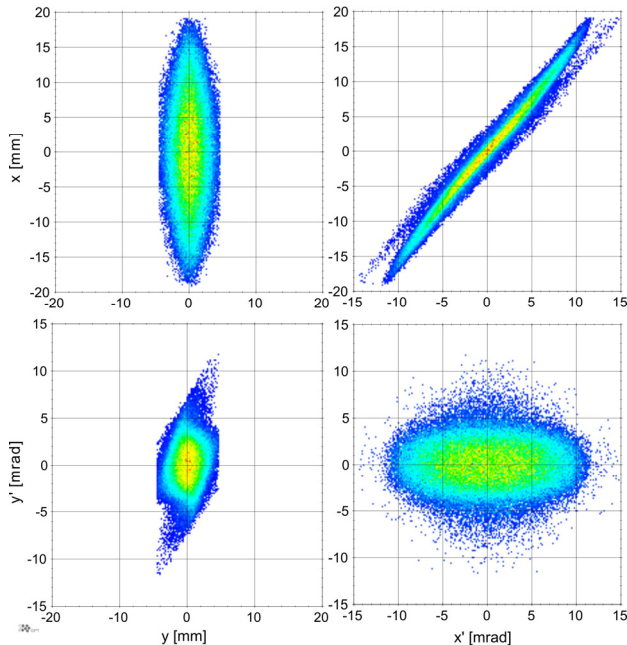


Figure 3: Particle distribution at position 4.13 m behind the RFQ exit used for the following simulations as input.

The presented results have then been produced for each lattice variation in 3 different steps. In the first step the dipole was assumed to be switched off and the particle tracking into the main beam dump was simulated. The

second step was the simulation of the particle transport into the second beam dump assuming the dipole field is switched on. This simulation also produced the particle distribution at the point of interaction with the laser beam as input for the final step. In the third step the particles were tracked from the laser interaction point to the particle detector. In this last step of simulations either the full beam distribution was tracked, or by introduction of a slit aperture, a sequence of “ribbon” beams of variable width, similar to the ones produced by the laser, could be simulated. Figure 4 presents a trajectory plot of all 3 simulations combined.

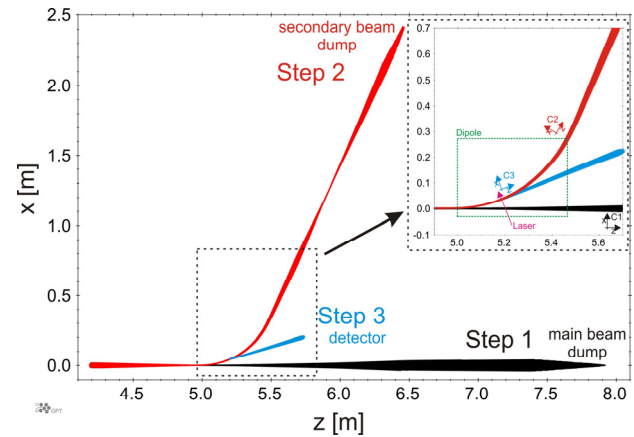


Figure 4: Trajectory plots for all three steps of the simulations combined. While in step 1 no change of coordinate system (C1 see insert) is required. For convenience the beam leaving the dipole in step 2 is referenced to coordinate system C2. The beam of neutralized particles after the laser interaction (step 3) is given in the coordinate system C3.

PARTICLE TRANSPORT SIMULATION RESULTS

Following a summary of the particle tracking results from a large number of simulations is given. Figure 5 and 6 show the distribution of the particle beam in the transversal direction for different z positions when the dipole is off (Fig. 5) and the dipole is on (Fig. 6). Without dipole field the beam distribution is nearly homogeneous and divergent in both transversal planes.

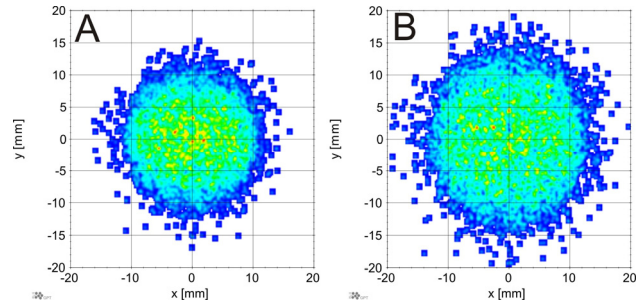


Figure 5: Plots show the particle distribution at the exit (A) and 0.5 m behind the exit of the dipole (B) in direction of the main beam dump.

Copyright © 2013 by JACoW — cc Creative Commons Attribution 3.0 (CC-BY-3.0)

Due to the weak focussing of the dipole in the x direction, the beam size in direction of the second beam dump is significantly smaller (in x) than towards the first dump. Additionally a focal spot can be observed (in x) between position A and B. As this effect cannot be avoided the lattices following the dipole will be different to accommodate for this effect.

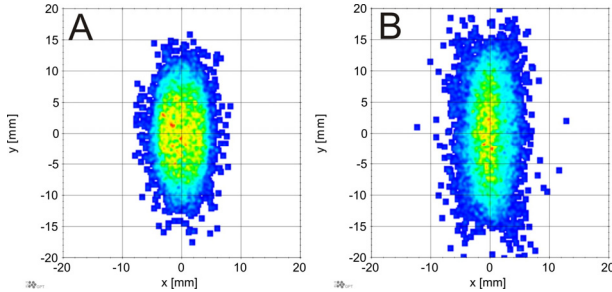


Figure 6: Plots show the particle distribution at the exit (A) and 0.5 m behind the exit of the dipole (B) in direction of the second beam dump (C2 coordinate system). In comparison with Fig. 5, the influence of weak focussing of the dipole on the beam distribution in x is clearly visible.

Particle Tracking to the Particle Detector

In Fig. 7 one example for the particle tracking from the interaction point with the laser towards the particle detector is shown for two different y-position of the laser in respect to the ion beam (+3 mm and 0 mm).

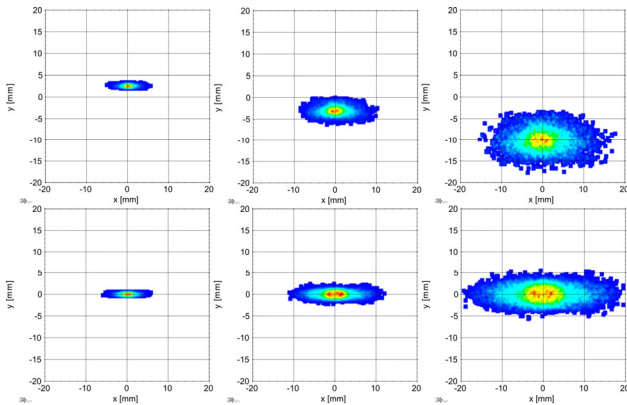


Figure 7: Upper plots show the development of the neutralized particle distribution as a function of the distance to the laser interaction point (left to right : $z=0\text{mm}$, $z=370\text{mm}$, $z=800\text{mm}$, C3 coordinate system) for a laser position $y=+3\text{mm}$, lower plots for the same positions but the laser at $y=0\text{mm}$.

While the movement of the centre of gravity and the developing spread in the y direction from the width of the laser (in $z=0\text{mm}$) directly allows to determine the y, y' emittance using different laser positions, a detector movable in the z direction will also offer the possibility to investigate the x, x' phase space simultaneously. For FETS it is planned to allow for a scintillator movement between 0.4 and 0.7 m behind the laser interaction point, in a

second phase of the setup. Furthermore it is planned to allow for a focus of the laser beam in the interaction region as an additional parameter for improved data reconstruction.

Influence of Dipole Fringe Fields

To evaluate the influence of the fringe field of the LD dipole on the particle transport, the hard edge assumption of the dipole field has been replaced by the use of an Enge function to describe the fringe fields produced by the dipole. Two distributions of the fringe field for different parameters of the Enge function are shown in Fig. 8. The expected real function of the fringe field was very recently evaluated using a full 3D map produced by the OPERA code (green dashed line in Fig. 8). For the following simulation results the parameters $d1=0.04$ and $b1=50$ were chosen, which should reproduce the real effect of the fringe field reasonably well.

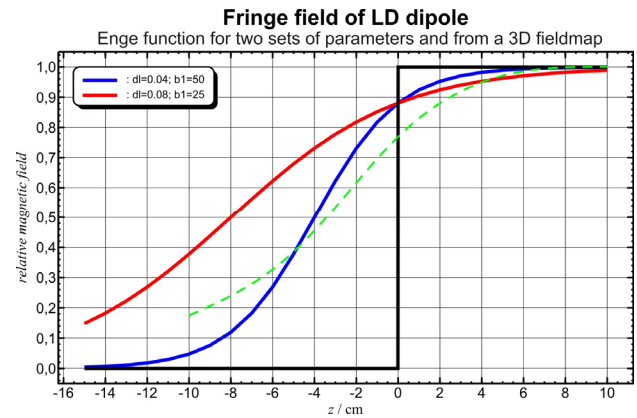


Figure 8: Dipole fringe fields calculated using Enge functions (red, blue) in comparison with the result of a recent 3D simulation using OPERA (green).

Compared with the simulation using a hard edge dipole field distribution (Fig. 9 a) in the following the peak magnetic field was reduced by a factor of 0.874 to achieve the same integrated field and correcting for the additional influence of the fringe fields on the beam transport (Fig. 9b).

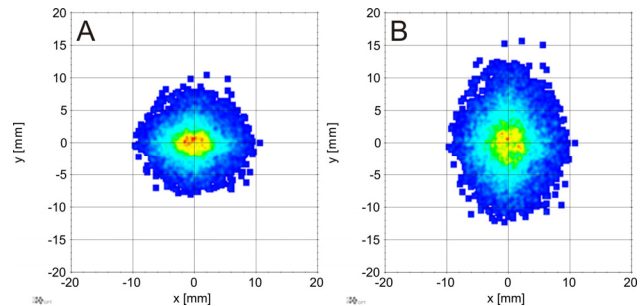


Figure 9: Left plot (A) shows the particle distribution at the exit of the dipole in direction of the second beam dump (C2) without fringe fields, the right plot (B) shows the distribution at the same position with fringe fields included. In plot B the maximum field strength was adjusted to produce the same integrated field.

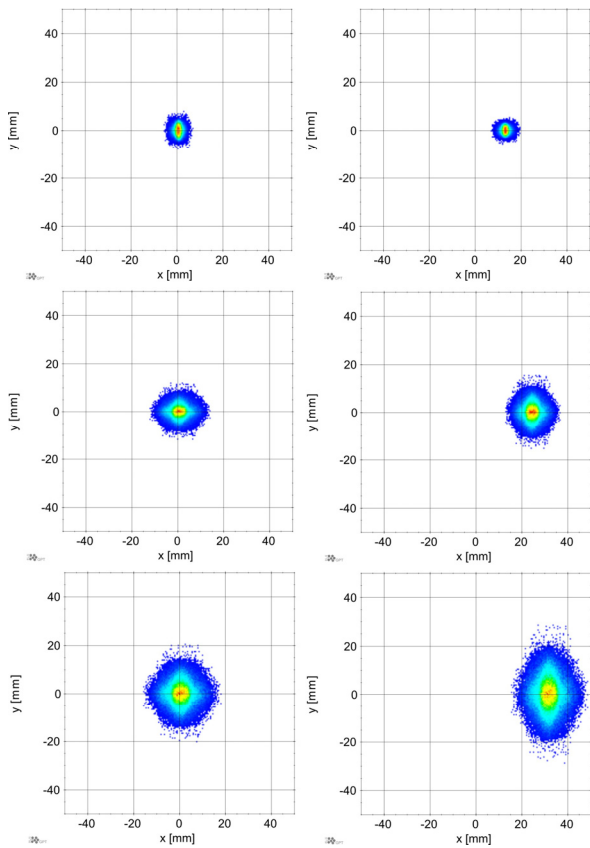


Figure 10: Left plots show the particle distribution of the neutralized particles (C3) without, right plots with fringe field effects. Upper row show the distributions at the laser interaction, second row at the exit of the laser diagnostic vessel and lower row 0.6m behind the laser interaction.

While for the beam into the secondary beam dump the effect of the fringe fields can be corrected by reducing the peak magnetic field, this is not simultaneously valid for the neutralized particles as shown in Fig. 10. Following a more rigorous analyses of the data, a redesign of the LD vessel to accommodate for this effect will be required.

SUMMARY AND OUTLOOK

A framework of simulations has been setup in GPT. The output of previous MEBT simulations was used together with a realistic description of the laser diagnostic setup to perform first simulations of beam transport in the laser diagnostic vessel. Preliminary results are:

- 1) As without a following DTL a rebunching cavity is not necessarily required and the open diameter of the cavity severely limits the acceptance of the experimental setup a bunching cavity in front of the diagnostic vessel will not be incorporated in the first experiments.
- 2) To further increase the available acceptance of the setup, longer quadrupoles with larger bore radius (50 mm compared to 38 mm in the MEBT) will be used.
- 3) A detector (diameter ~ 90 mm) moveable in position from ~ 0.4 - 0.7 m behind the laser interaction point seems most attractive in terms of resolution and range.

4) Due to weak focussing of the beam by the dipole; the additional use of edge focussing is considered.

5) While the effect of the dipole fringe fields can be corrected for the beam in the direction of the second beam dump, this is not possible for the particles that will be neutralized. This effect requires a redesign of the diagnostic vessel, but needs also be considered in the reconstruction of the beam emittance. The next steps of investigations will include:

- Further variation of QP positions and settings to allow for highest phase space sampling.
- Investigate power distribution on beam dumps.
- Investigate optimum for laser size and stepping in y.
- Determination of neutralisation yield, calculation of expected scintillator output and subsequent the expected signal strength in the CCD camera.

ACKNOWLEDGMENT

The authors would like to thank Peter Savage for the technical drawings and Dan Faircloth for the data from the 3D OPERA simulations.

REFERENCES

- [1] D.J.S. Findlay et al, "The RAL Front End Test Stand", Proc. NuFact04, Osaka University, Japan, Aug 2004.
- [2] A. Letchford et al, "Status of the RAL Front End Test Stand", IPAC2013, Shanghai, May 2013.
- [3] D. C. Faircloth et al, "The front end test stand high performance H- ion source at Rutherford Appleton Laboratory", Rev. Sci. Instrum. 81, 02A721 (2010).
- [4] J. J. Back et al, "Commissioning of the Low Energy Beam Transport of the Front End Test Stand", IPAC2010, Kyoto, May 2010.
- [5] P. Savage et al, "Production of the FETS RFQ", IPAC2013, Shanghai, May 2013.
- [6] M. Aslaninejad et al, "MEBT design for the Front End Test Stand project at RAL", IPAC13, Shanghai, May 2013.
- [7] M. Clarke-Gayther, "A Two Stage Fast Beam Chopper for Next Generation High Power Proton Drivers", IPAC2011, San Sebastian, September 2011.
- [8] C. Gabor, O. Meusel, J.K. Pozimski, Status report of the Frankfurt H- LEBT including a non-destructive emittance measurement device, Proc. of 9th Internat. Sym. of PNNIB, 2002, CEA/ Saclay, Paris, France.
- [9] C. Gabor, H.Klein, O.Meusel, U.Ratzinger, J.K.Pozimski, "Experimental results of a non-destructive emittance measurement device for H- beams", PAC05, Knoxville, Tennessee, USA, May 2005.
- [10] C. Gabor et al., "Laser-based Beam Diagnostic for the Front End Test Stand (FETS) at RAL", TUPCH019, EPAC'06, Edinburgh, June 2006, <http://www.JACoW.org>.
- [11] D. Lee et al., "A laserwire beam profile measuring device for the RAL Front End Test Stand", TUPB11, DIPAC'07, Venice, May 2007, <http://www.JACoW.org>.
- [12] D. A. Lee et al., "Laser-based Ion Beam Diagnostics for the Front End Test Stand at RAL", TUPC058, EPAC'08, Genoa, June 2008, <http://www.JACoW.org>.
- [13] Pulsar Physics, <http://www.pulsar.nl/gpt>.